

# Crushtaceans and Complements of Fully Augmented and Nested Links

Matthew Zevenbergen

May 2021

## Abstract

This paper addresses fully augmented links (FALs) and nested links, two subclasses of generalized FALs. We utilize a graph called the crushtacean, which is derived from a cell decomposition of the link complement. Applications are made to fully augmented pretzel links, including describing a sequence of Dehn twists to generate a family of nested links with homeomorphic complements; the size of this family is shown to grow exponentially with the number of link components. We also prove that the fully augmented pretzel links are determined by their complements, within the class of FALs.

## 1 Introduction

Fully augmented links are a class of hyperbolic links that have been studied because of their geometric properties. Nested links are a generalization that preserve most of these properties. We introduce these classes of links and some related structures in Section 1.

Gordon and Luecke have famously proven that knots are determined by their complements [4]. This is not the case for links, for example Whitehead has shown that there are infinitely many links with the same complement as the Whitehead link [14]. There are some common questions that one can ask about link complements. Magnum and Stanford state a few of these questions in [7], where they also prove that Brunnian links are determined by their complements.

The first question is “For a given link (or family of links)  $L_1$ , can we characterize the links  $L_2$  such that  $S^3 \setminus L_1$  is homeomorphic to  $S^3 \setminus L_2$ .” In Section 2, we address this by providing a sufficient condition for the complement of a nested link to be homeomorphic to the complement of a fully augmented link. In Section 3.1, we also look at a subclass of fully augmented links called fully augmented pretzel links, and describe a family of nested links that have the same complement. We show that the size of this family grows exponentially with the number of components of the fully augmented pretzel link.

A second question that Magnum and Stanford ask is “Can we characterize those links that are determined by their complements?” In Section 3.2, we prove that within the class of fully augmented links, the fully augmented pretzel links are determined by their complements.

### 1.1 Fully Augmented and Nested Links

In this paper, we will discuss two related classes of hyperbolic links called *fully augmented links* (FALs) and *nested links*. We’ll introduce these here, but a more thorough introduction is given in [10] and [9]. To construct a fully augmented link, start with a link diagram and around each twist of two strands, place an unknotted component. Then, remove all full twists from the twist region, leaving either no twist or a half twist, as in Figure 1.

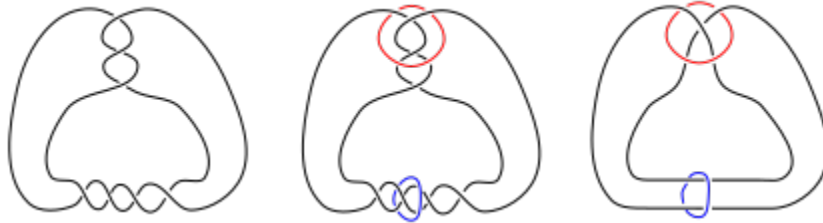


Figure 1: Left: A link diagram. Center: Placing unknotted components around twist regions. Right: Removing all full twists, creating an FAL.

Nested links, as discussed in [9], are a generalization of fully augmented links. Twist regions will be allowed to have more than two strands if we can add unknotted components around the twist region in such a way that every unknotted component bounds a twice punctured disk, where these punctures may be strands in a twist or other unknotted components. Notice that the term nested comes from the fact that if one of the punctures in such a disk comes from an unknotted component, then that component must bound another twice punctured disk. An example of this process is given in Figure 2.

For both FALs and nested links, we’ll call the added unknotted components *crossing circles* and we’ll call all other components *knot circles*. We’ll call the twice punctured disks that are bounded by the crossing circles *crossing disks*. If there is a half twist between the two strands that puncture a crossing disk, we will say that that crossing region is *twisted*, and *flat* otherwise. In some circumstances we’ll discuss nested links with twisted crossing regions, but the majority of our discussion will be concerning nested links where every crossing region is flat, which can be simply called flat nested links or FALs.

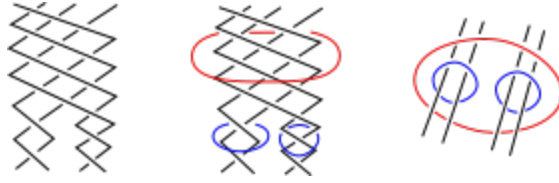


Figure 2: Left: A twisted tangle. Center: Placing unknotted components around twist regions. Right: Removing all full twists.

## 1.2 Cell Decomposition

A link  $L$  is hyperbolic if its complement  $S^3 \setminus L$  admits a hyperbolic structure. This hyperbolic manifold may be decomposed into a collection of polyhedra with associated instructions for gluing the faces. We examine a method of finding a cell decomposition of the link complement, as described in [9]. The method for FALs is a subcase. Figure 3 depicts the steps.

First, position the link so that all knot circles lie in a single plane and every crossing disk is perpendicular to that plane. Then, we cut along this plane, creating two symmetric regions above and below this plane which we'll call  $P_+$  and  $P_-$  respectively. We'll continue only looking at one of these regions, since the other is symmetric and handled identically. Now, slice along the crossing disks, colored gray in the figure, keeping track of what faces are glued. We then flatten these disks into the plane, as in the second part of Figure 3. Then, shrink the arcs corresponding to crossing circles, as in the third part of the figure. Finally, shrink the arcs corresponding to the knot circles.

With each  $P_+$  and  $P_-$  we can associate an ideal polyhedron. The vertices of these polyhedron will be the vertices in the cell decomposition and the faces will correspond to the shaded and unshaded regions in the decomposition. A reader interested in this cell decomposition is referred to [10] and the appendix in [6] by I. Agol and D. Thurston for more details.

## 1.3 Crushtaceans

From the cell decomposition described in Section 1.2, we can obtain a graph which Chesebro, DeBlois, and Wilton call the *crushtacean* [1]. To form this graph, place a vertex in the center of each shaded region of the cell decomposition of  $P_+$  (or  $P_-$ ) then add an edge connecting vertices corresponding to adjacent shaded regions. This is depicted in Figure 4 where we continue the example from Figure 3. The crushtacean is the dual graph to what is referred to as the nerve by Purcell [10].

We'll now examine some combinatorial properties of the crushtacean. For our purposes, a *simple* graph is one where each edge has distinct endpoints and no two vertices are joined by more than one edge. Additionally, a *trivalent* graph is one

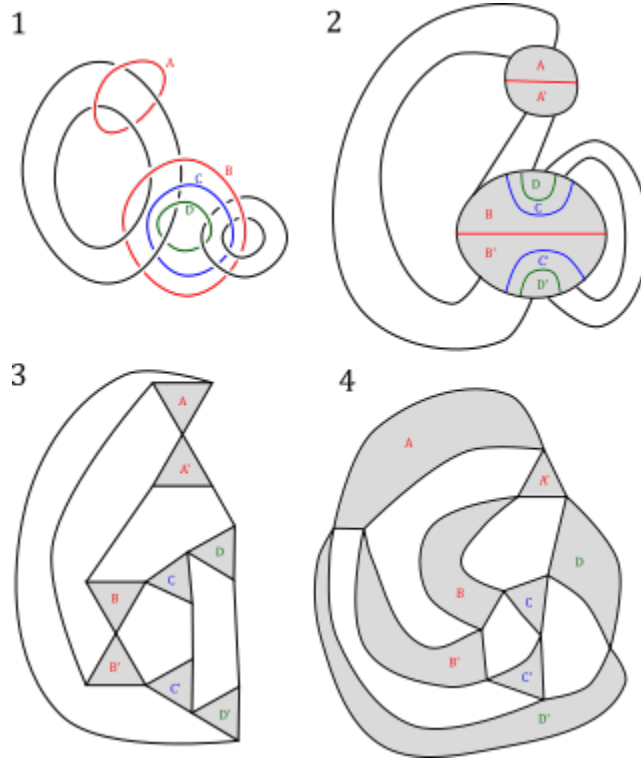


Figure 3: The cell decomposition process for a nested link complement.

where every vertex has degree three. A graph is *maximal planar* if it is simple and planar, but adding any edge would destroy one of these properties.

A *triangulation of  $S^2$*  is a simple planar graph with at least two faces such that each face has three edges and no distinct faces share more than one edge. Purcell proves in [10] that the crushtacean is the dual graph to a triangulation of  $S^2$ . We now investigate combinatorial properties of spherical triangulations, which combine with duality to reveal similar structure in crushtaceans.

**Lemma 1.3.1.** *Let  $\Gamma$  be a triangulation of  $S^2$ . Then,  $\Gamma$  has at least 4 vertices and is maximal planar.*

*Proof.* Let  $\Gamma$  be a triangulation of  $S^2$ . Since  $\Gamma$  is simple, if  $\Gamma$  had fewer than three vertices, then  $\Gamma$  must have fewer than two faces. Thus,  $\Gamma$  must have at least three vertices. Now, suppose  $\Gamma$  has exactly three vertices. Then, since it is simple, planar, and must have more than one face,  $\Gamma$  must form a triangle, splitting  $S^2$  into exactly two faces. These two faces must share more than one edge. This is a contradiction, so  $\Gamma$  must have more than three vertices. This proves the first half of our statement.

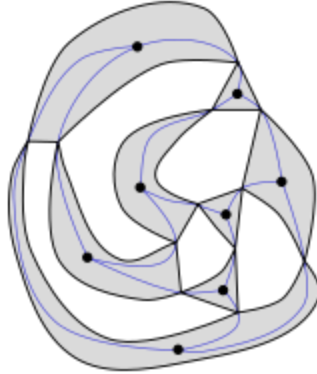


Figure 4: Constructing a crushtacean.

To add any edge to  $\Gamma$  while maintaining planarity, we must add an edge through a face. Since each face of  $\Gamma$  is a triangle, however, if vertices  $u$  and  $v$  share a face, then  $u$  and  $v$  must also be adjacent. Thus, we cannot add any edges to  $\Gamma$  while maintaining both planarity and that  $\Gamma$  is simple, so  $\Gamma$  must be maximal planar.  $\square$

A graph  $G$  is  $k$ -vertex-connected if  $G$  has more than  $k$  vertices and remains connected when any collection of fewer than  $k$  vertices are removed. It is a common fact, stated in [3], that maximal planar graphs with at least four vertices are 3-vertex-connected. We have then shown that any triangulation of  $S^2$  is 3-vertex connected. A 3-vertex connected, simple, planar graph is also known as a *polyhedral graph*.

**Proposition 1.3.2.** *The crushtacean of a hyperbolic nested link is 3-vertex-connected, simple, planar, trivalent graph.*

*Proof.* Let  $\Gamma$  be the crushtacean of a hyperbolic nested link. Since the upper half of each twice punctured disk in the cell decomposition has three edges, we know each shaded region of the decomposition will be a triangle. Then, since we connect vertices of  $\Gamma$  through the corners of these shaded regions, each vertex must be degree three.

In [10], Purcell proves that the crushtacean must be the dual graph of a triangulation of  $S^2$ , which we have shown must be a polyhedral graph. The dual to a polyhedral graph is unique, by [15], and is also a polyhedral graph. Thus, the crushtacean must be 3-vertex-connected, simple, planar, and trivalent.  $\square$

#### 1.4 Balanced Spanning Forests

We'll discuss one more structure related to the crushtacean. First, recall that a tree is a connected graph that has no cycles and a forest is a collection of trees.

A *balanced tree* is a tree that admits an involution that fixes one edge,  $e^*$ . This involution induces a coloring such that edges mapped to one another have the same color. We'll refer to the edge  $e^*$  as the *edge of symmetry*. Now, given a graph  $G$ , a *balanced spanning forest* on  $G$  is a collection of disjoint balanced trees in  $G$  such that every vertex of  $G$  lies in some tree in this forest.

From the cell decomposition of the complement of a nested link, we can find a unique balanced spanning forest on the crushtacean. This will be constructed in such a way so that vertices mapped to each other by the involution correspond to a pair of faces that are glued in the cell decomposition. This is shown in Figure 5. The existence this balanced spanning forest follows from the construction of the cell decomposition. We'll refer to the structure of a crushtacean with a balanced spanning forest on it as a *painted crushtacean*.

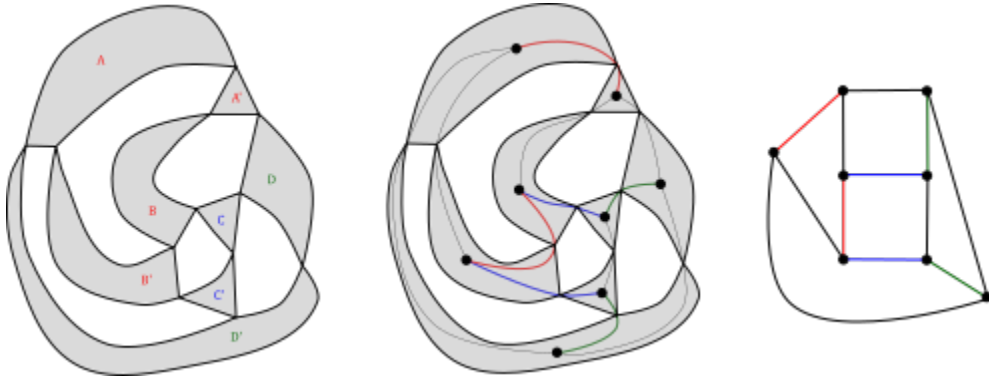


Figure 5: Left: A cell decomposition. Center: A balanced spanning forest on a crushtacean. Right: This crushtacean separate from the cell decomposition.

We now state a proposition proven by Harnois, Trapp and Olsen in [5].

**Proposition 1.4.1.** *Let  $G$  be a simple, planar, trivalent, 3-vertex-connected graph. Then, for each balanced spanning forest on  $G$  there is a hyperbolic nested link for which this is the painted crushtacean. Further, there is a unique nested link with this property if we require every crossing disk punctured by two knot strands is flat.*

Note that in [5], this proposition is stated requiring that  $G$  be the dual of a triangulation of  $S^2$ , but the equivalence of these statements follows from Lemma 1.3.1 and the fact that the dual of a 3-vertex-connected graph is 3-vertex-connected.

We conclude this section with some definitions. A *matching* of vertices refers to a tree composed of one edge. A balanced spanning forest where every tree is a matching is called a *perfect matching*. The balanced spanning forest corresponding to an FAL will be a perfect matching. Perfect matchings have been extensively explored in the context of planar trivalent graphs, for example in [2]. We will say

that a pair of vertices in a crushtacean are *glued* if they are mapped to one another by the involution on a balanced tree, in connection to the corresponding faces in the cell decomposition being glued. The *gluing pattern* refers to the collection of information about which vertices are glued. Finally, a pair of vertices will be said to be *glued by* a tree or forest if they are glued in the induced gluing pattern.

## 2 Nested Links with the Complement of an FAL

This section focuses on describing a sufficient condition for the complement of a nested link to be homeomorphic to that of a fully augmented link. Subsection 2.1 provides a brief introduction to Dehn twists in the context of link complements. Subsection 2.2 describes conditions for the gluing pattern on a nested link painted crushtacean to be the same as that for an FAL painted crushtacean. In cases where the gluing pattern is the same, a homeomorphism between the complements of these nested links and FALs is then described. Subsection 2.3 introduces a family of crushtaceans called *generalized ladder graphs* that have the properties described in Subsection 2.2. A complete description of this family is given.

### 2.1 Dehn Twists

As previously mentioned, Whitehead has shown that there are infinitely many non-isotopic links with the same complement as the Whitehead link [14]. The Whitehead link is shown in the left-most image of Figure 6, and the remaining links shown in Figure 6 are a few examples of links with homeomorphic complements, as Whitehead constructed.

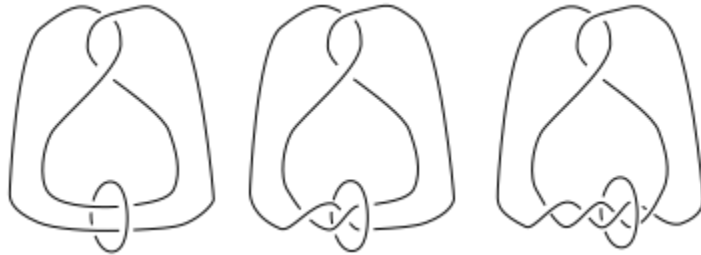


Figure 6: The Whitehead link and some links with the same complement.

We'll discuss, with some level of informality, Whitehead's construction in more generality. More details are given in [11]. Suppose in a given link  $L$  we have an unknotted component  $C$  that does not cross itself, as in the Whitehead link. The complement  $S^3 \setminus C$  is a solid torus, and the remainder of the link lies in this solid torus. Note that the component  $C$  bounds a disk  $D$  in  $S^3 \setminus C$ . Now, the main step

in Whitehead's construction is to slice along such a disk  $D$ , rotate one full time, and then re-glue the disk, as is shown in Figure 7. This process of slicing along a disk bounded by an unknotted component, rotating one full time, and regluing is called a *Dehn twist*. Intuitively, one can think of this process as adding one full twist between the strands that pass through  $C$  and puncture  $D$ . As they have been described, a Dehn twist is a homeomorphism between link complements, as is discussed in [11].

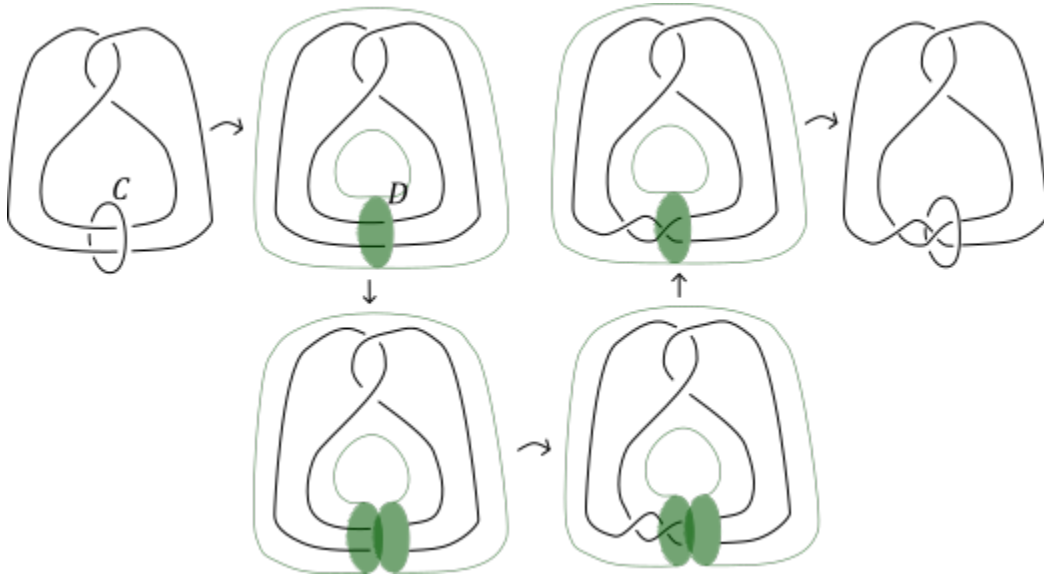


Figure 7: The steps of a Dehn twist.

## 2.2 Ladder Subgraphs of Crushtaceans

Given a link  $L$ , its complement  $S^3 \setminus L$  is a 3-manifold. If a link  $L^*$  is isotopic to  $L$ , then  $S^3 \setminus L$  is homeomorphic to  $S^3 \setminus L^*$ , but the converse is not necessarily true.

Our goal is to address when nested links and fully augmented links have homeomorphic complements. The following Theorem concerning simple planar trivalent graphs will be useful in considering the question.

**Theorem 2.2.1.** *Given a simple trivalent graph with a balanced spanning forest, there exists a perfect matching that induces the same gluing pattern if and only if all vertices are glued to an adjacent vertex in the gluing pattern induced by the forest.*

*Proof.* If the vertices glued by the balanced spanning forest are not adjacent, then no perfect matching can induce the same gluing pattern, as all vertices glued by a perfect matching are adjacent.



Now, to address the converse, we suppose that all pairs of glued vertices are adjacent. We'll show that the collection of these edges of adjacency between glued vertices give a perfect matching on the graph. First, notice that none of these edges of adjacency can share a vertex, as every vertex is glued to exactly one other. Second, since every vertex is glued to another, this collection of disjoint edges span the vertices of the graph, hence is a perfect matching.  $\square$

Now, we want to introduce a certain type of graph called a *ladder graph*, denoted  $L_n$ , with  $2n$  vertices and  $3n - 2$  edges. We depict  $L_5$  and the general structure of  $L_n$  in Figure 8. We'll call the edges of the type that are depicted as vertical in

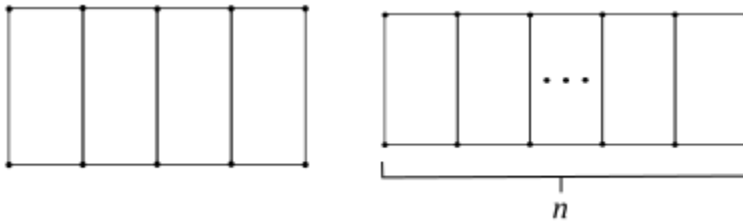


Figure 8: Left: Ladder Graph,  $L_5$ . Right: Ladder Graph,  $L_n$ .

Figure 8 the *rungs* of the ladder, and the other edges will be the *rails*. We want to consider ladder graphs as subgraphs of crustaceans. The perfect matching on a ladder graph given by coloring all the rungs of the ladder will be referred to as the *canonical* perfect matching on this ladder.

**Proposition 2.2.2.** *Let  $\mathcal{F}$  be a balanced spanning forest on a crustacean  $G$  that induces the same gluing pattern as the perfect matching  $M$ . Let  $E$  be the set of edges that do not lie in  $M$  or  $\mathcal{F}$ . Then, either*

1.  $G$  is  $K_4$  or
2. the graph  $G' = G \setminus E$  is a disjoint union of ladder graphs.

*In the second case, each ladder must be spanned by a single balanced tree of  $\mathcal{F}$  for which the edge of symmetry is one of the rungs of the ladder, and the other edges must be the rails of the ladder.*

*Proof.* We consider the subgraph spanned by one tree in  $\mathcal{F}$  with more than one edge. First, we note that one of the edges in  $M$  on this subgraph must be the edge of symmetry for our balanced tree, since the edge of symmetry glues adjacent vertices and  $\mathcal{F}$  induces the same gluing pattern as  $M$ . The rest of the proof will be determining the structure of the remainder of this subgraph and the accompanying balanced tree.

The edge of symmetry that is also in the perfect matching is colored red in Figure 9. In this diagram, we have colored one adjacent edge blue to represent the continuing tree. This tree must be balanced, so we must also color either  $e_1$  or  $e_2$  blue. We'll look at these as two separate cases.

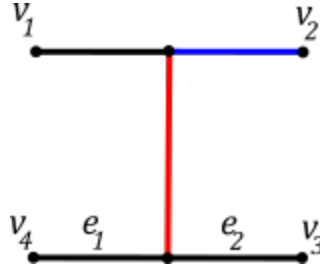


Figure 9: An edge of symmetry with one adjacent edge colored.

*Case 1:* Assume we color  $e_1$  blue. This tree must then glue the vertices  $v_2$  and  $v_4$ , but then our hypothesis and Theorem 2.2.1 tell us that there must be an edge between  $v_2$  and  $v_4$ , as depicted in the first diagram of Figure 10. Now, we have two subcases: either  $v_1 \neq v_4$  or  $v_1 = v_4$  (where equality here means that they are the same point).

If  $v_1 \neq v_4$ , then there must be some subgraph  $T$  that  $v_1$  is connected to, as shown in the second image of Figure 10. Then since our graph must be 3-vertex connected, by Proposition 1.3.2, there must be an edge connecting  $T$  to each of  $v_2$  and  $v_4$ , else there would be two vertices that we could remove and disconnect  $T$  from the rest of the graph (also noting that our graph must be planar). Then, however, since every vertex has degree 3, the crusetacean must be of the form in the third diagram of Figure 10, so removing the edge  $e_2$  disconnects our graph, so the crusetacean is not 3-vertex-connected. Thus, we cannot have  $v_1 \neq v_4$ .

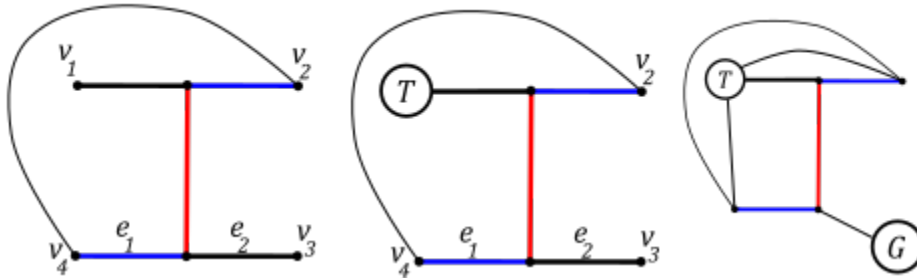


Figure 10: Addressing the case where  $e_1$  is colored and  $v_1 \neq v_4$ .

Then, if  $v_1 = v_4$ , we must also have  $v_3 = v_2$ , as in the first diagram of Figure 11. This follows since every other existing vertex is already degree 3, so there must be

some subgraph  $G$  that would be disconnected from the crushtacean by removing  $v_2$  and  $v_5$ , as in the second diagram of Figure 11, which would again contradict that the crushtacean is 3-vertex-connected. Thus, in this case, our crushtacean must be  $K_4$ .

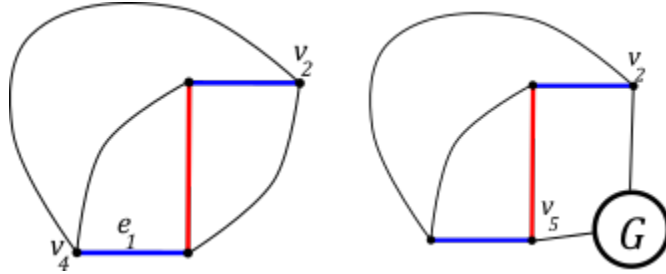


Figure 11: Addressing the case where  $e_1$  is colored and  $v_1 = v_4$ .

*Case 2:* Now, assume we color  $e_2$  blue. Then, since our glued vertices must be adjacent, there must be an edge connecting  $v_2$  and  $v_3$ , as in the first diagram of Figure 12. Now, if we extend the forest from the end of the blue edges, we must color both  $e_3$  and  $e_4$ , to maintain balance, and there must be an edge between the endpoints of these edges, since we want glued vertices to be adjacent. This is depicted in the second diagram in Figure 12.

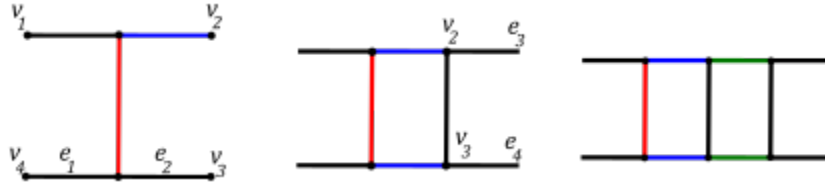


Figure 12: Construction of a ladder subgraph.

We can extend this argument to show that, in this case, if we have a balanced tree such that all vertices are glued to an adjacent vertex, then the tree and this portion of the crushtacean must have this structure shown in Figure 13, where the sections labeled  $A$  and  $B$  may each contain arbitrarily many pairs of colored edges. Note that the subgraph spanned by this tree is indeed a ladder graph. Further, the edge of symmetry of this tree is a rung of the ladder and all other edges are rails.

We can see that in this second case, all the edges that are in either  $M$  or  $\mathcal{F}$  are in one of the subgraphs spanned by a tree in  $\mathcal{F}$ , which we showed must be a ladder graph.  $\square$

With a given ladder and balanced forest on this ladder we can associate a tangle, which will be part of the nested link associated with the crushtacean. Figure 14 gives

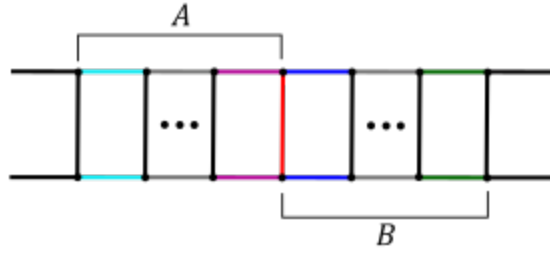


Figure 13: A large ladder.

some examples for a ladder with two rungs. Note that in general, a ladder with  $n$  rungs with the canonical perfect matching will correspond to a chain with  $n$  crossing circles. Figure 15 depicts this, along with the same ladder and an arbitrary balanced tree that gives the same gluing pattern.

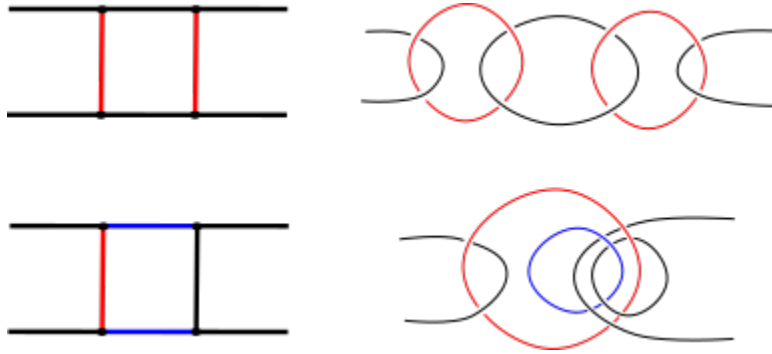


Figure 14: Top: A two rung ladder with the canonical perfect matching and the associated tangle. Bottom: A two rung ladder with a single balanced tree that gives the same gluing pattern as above and the associated tangle.

**Theorem 2.2.3.** *If a fully augmented link  $F$  and a nested link  $N$  have the same crusstacean, other than  $K_4$ , with the same gluing pattern, then there is a homeomorphism  $h : S^3 \setminus F \rightarrow S^3 \setminus N$  given by a sequence of Dehn twists.*

*Proof.* By Proposition 2.2.2, the balanced forest associated with  $N$  must only differ from the perfect matching associated with  $F$  on a set of ladder subgraphs, on each of which a single balanced tree gives the same gluing pattern as the perfect matching. Since modifying a balanced spanning forest on a single ladder has only a local effect on the associated link, we'll assume without loss of generality that the balanced forest associated with  $N$  only differs from the perfect matching associated

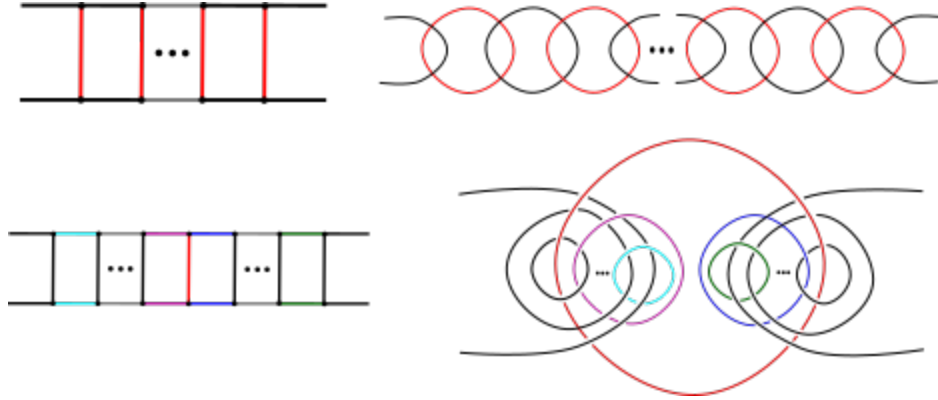


Figure 15: Top: An  $n$  rung ladder with the canonical perfect matching and the associated tangle. Bottom: An  $n$  rung ladder with a single balanced tree that gives the same gluing pattern as above and the associated tangle.

with  $F$  on a single ladder. The more general case will be a composition of such homeomorphisms.

First, notice that we can also describe  $h$  as a composition of homeomorphisms  $h_i$  between the complements of nested links corresponding to iteratively removing one perfect matching edge from the forest and extending the balanced tree on this ladder by two rail edges that will then glue the same vertices as the removed edge.

Now, note that each homeomorphism  $h_i$  will be isotopic to the identity everywhere except the region local to the tangle associated with this ladder, since the links  $F$  and  $N$  must be identical on all other regions. We'll now proceed inductively, to show that each  $h_i$  is given by a sequence of Dehn twists.

The base case will be replacing two rungs of a ladder with a balanced tree that gives the same gluing pattern, as is depicted in Figure 14. By symmetry, examining this case will also suffice to address the case where the edge of symmetry is on the right of the colored rails. We will now use Figure 16 to depict the sequence of Dehn twists that will give the homeomorphism  $h_1$ . The first image in this figure gives a sublink of  $F$  as follows: for our current purposes, the green torus represents the left crossing circle in the top image in Figure 14. It suffices to look at this sublink because we will only perform Dehn twists about the components that are blue and red in Figure 16, and we have included all components that are linked with these components.

In the second image, we perform a single Dehn twist about the red component, which is punctured by the green and blue components. In the third image, we perform a twist about the blue component, which is currently punctured by the red, green, and black components. Notably, this unlinks the green and red components,

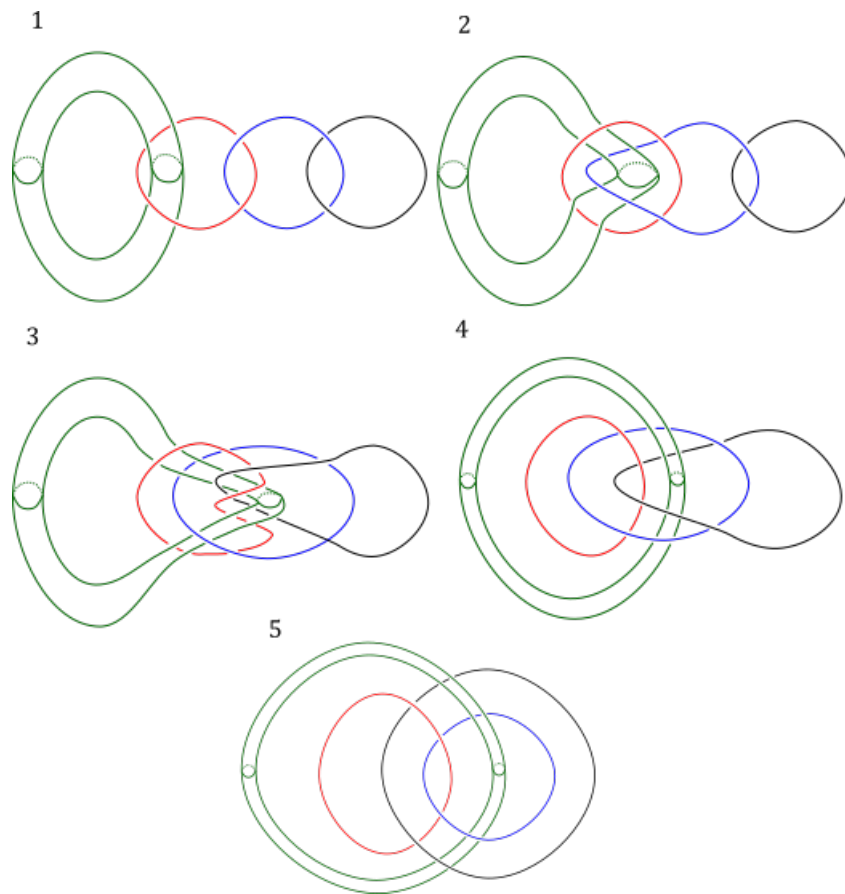


Figure 16: The Dehn twists described in the proof of Theorem 2.2.3.

and we perform an isotopy in the fourth image to emphasize that these components are indeed unlinked. Finally, in the fifth image, we do a single Dehn twist about the red component, which unlinks the black and the blue components. One can then confirm with Figure 14 that the result of these Dehn twists matches the expected tangle.

Now, assume  $h_i$  is given by a sequence of Dehn twists for  $1 \leq i \leq n$ . We'll show that  $h_{n+1}$  is also given by Dehn twists. We'll again assume that the tree is being extended on the right side, and the other case will be given by symmetry. We will again reference Figure 16 (however the green torus will be interpreted differently in this step). The sublink we'll look at this time is given in Figure 17. It will suffice to look at this sublink because we have included all components that link with circles  $u$  and  $v$ , which will be the only components that we perform Dehn twists about. In this case, we'll take the meridian of the green torus to be the knot circle labeled

$c$  that lies in the plane. The torus will then encompass the crossing circles that appear green, blue, and red in Figure 17, in addition to those that lie in the ellipsis. The red and blue components in Figure 16 will correspond to those labeled  $u$  and  $v$  in Figure 17, respectively.

We will again start by performing one Dehn twist about the red component. Now, however, the components contained in the green torus will become twisted with one another, but this is not the desired effect, so we perform an additional Dehn twist, in the opposite direction as the last one, about the meridian of the green torus. This untwists the components contained inside. We then continue along as before, but every time we perform one of the depicted Dehn twists, we must perform an additional one in the opposite direction about the meridian of the green torus, to untwist the components contained inside. After this process, we can confirm that the result depicted in the fifth image of Figure 16 is indeed the expected local structure of this link.

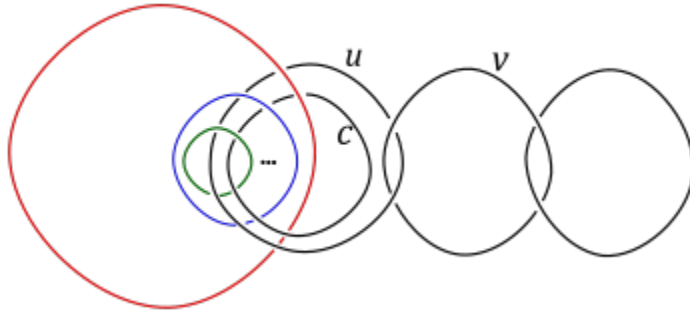


Figure 17: The sublink we'll look at for addressing the homeomorphism  $h_{n+1}$ .

In this way, we can give a sequence of Dehn twists that combine to give a homeomorphism between  $S^3 \setminus F$  and  $S^3 \setminus N$ .  $\square$

### 2.3 Generalized Ladder Graphs

We would now like to take a closer look at the crushtaceans and associated balanced forests that have a perfect matching inducing the same gluing pattern. Specifically, we want to consider crushtaceans such that we can replace a perfect matching with a balanced spanning forest consisting of trees that all have more than one edge, but induces the same gluing pattern as that perfect matching. It follows from Proposition 2.2.2 that each tree in this forest must span a subgraph given by the ladder graph,  $L_n$ , for some  $n \geq 2$ . Then, our crushtacean must have the structure of a collection of ladder graphs with additional edges attached to the degree two vertices in the ladders, which then connect these ladders. These additional edges will

be called *feet* (with the singular *foot*). An example of such a structure is depicted in Figure 18, where the feet are colored blue.

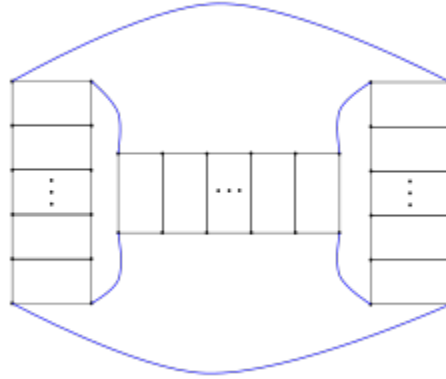


Figure 18: A crushtacean given by attaching a collection of ladders.

Notice that if we replace any ladder (with two or more rungs) with one with more rungs, our crushtacean will still have this property. For this reason, we will not presently distinguish between ladders with different numbers of rungs; we will just concern ourselves with the number of ladders in a crushtacean and how they are connected to one another.

A *generalized ladder graph* is given by connecting some number of ladders  $L_n$  of arbitrary length,  $n \geq 2$ , by some collection of feet such that the result must be a simple planar trivalent graph. We will also assume that all ladders in a generalized ladder graph are maximal, in the sense that there are no pairs of consecutive ladders that could be combined to form a larger ladder, as in Figure 19. The diagram in Figure 18 is an example of a generalized ladder graph. We now want to describe the set of generalized ladder graphs.

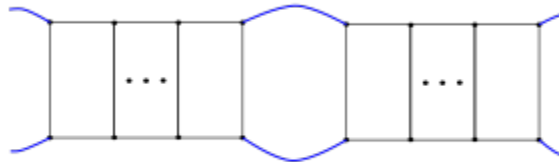


Figure 19: A disallowed subgraph of a generalized ladder graph.

First, we define a *bridge ladder* of a generalized ladder graph as a ladder that if



removed disconnects the graph. Similarly, we'll define a *bridge edge* of an arbitrary graph as an edge that if removed disconnects the graph.

**Lemma 2.3.1.** *A generalized ladder graphs with at least two ladders is 3-vertex connected if and only if no foot edge connects vertices that lie in the same ladder and there is no bridge ladder.*

*Proof.* First, suppose there is a foot of a generalized ladder graph that connects two vertices of the same ladder. We require that generalized ladder graphs be simple, so this foot must not connect two vertices that are already adjacent in the ladder itself. This must then happen as depicted in Figure 20. We notice, however, that since there is more than one ladder in our graph, the region labeled  $T$  is nontrivial. Thus, if we remove the two vertices circled in red, then our graph will become disconnected, so our graph is not 3-vertex-connected. Similarly, if there is a bridge

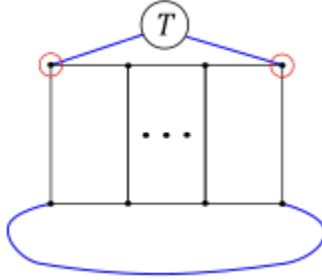


Figure 20: Subgraph of a generalized ladder graph where a foot connects two vertices in the same ladder.

ladder, then removing a pair of vertices that are endpoints of the same rung will clearly disconnect the graph.

Now, to address the converse, suppose every foot connects vertices in two distinct ladders and there is no bridge ladder. We'll show that in this case no pair of two vertices may be removed that disconnects our graph.

First, observe every ladder  $L_n$  is 2-vertex-connected ( $n \geq 2$ ). Thus, removing one vertex from two distinct ladders cannot disconnect our graph. Now, suppose we remove two vertices from the same ladder,  $L$ . If one or more of these are not attached to feet of a ladder and the graph becomes disconnected, then this ladder must be a bridge ladder.

The last case is removing two distinct vertices from  $L$  that are connected to feet. Note, however, that there will be two feet attached to  $L$  that are not affected by this removal. There is a path through  $L$  between these two feet and a path between every other vertex in  $L$  to each of these feet. Thus, since every foot connects two distinct ladders there is a path from every other ladder to one of these feet, our graph cannot be disconnected by removing two vertices.  $\square$

**Proposition 2.3.2.** *There is a bijection between the set of 3-vertex-connected generalized ladder graphs with more than one ladder and the set of perfect matchings on simple planar trivalent graphs without a bridge edge.*

*Proof.* Consider one colored edge,  $e$ , in a perfect matching on a simple planar trivalent graph without a bridge edge,  $G$ . Let  $v_*$  and  $v'$  be the endpoints of  $e$ . Let  $v_1$  and  $v_2$  be the other vertices adjacent to  $v_*$  and let  $v_3$  and  $v_4$  be the other vertices adjacent to  $v'$ . Now, we remove  $e, v_*$ , and  $v'$  from our graph. Then, we add in a ladder with an arbitrary number of rungs such that there is a foot connecting each of  $v_1, v_2, v_3$ , and  $v_4$  to one of the degree 2 vertices in our ladder so that  $v_1$  and  $v_2$  are adjacent and  $v_3$  and  $v_4$  are adjacent. This should be done so that these new edges don't cross; this will always be possible by switching the ladder vertex that an  $v_i$  is attached to, if necessary.

We then repeat this process for all edges in the perfect matching. The result will be planar and trivalent, by our construction. It will also be simple, because each ladder is simple and every foot edge must attach to two different ladders at different vertices. Since our initial graph,  $G$ , is also simple, there also cannot be any non-maximal ladders of the type shown in Figure 19. Thus, the result is a generalized ladder graph. Further, there must be at least two ladders in this graph, since  $G$  must have had at least two edges in its perfect matching. Then, since each foot edge connects two distinct ladders and there is also no bridge ladder, Lemma 2.3.1 tells us that our generalized ladder graph must be 3-vertex-connected.

Now, note that given a 3-vertex-connected generalized ladder graph, this process can be reversed to obtain a simple planar trivalent graph with a perfect matching, without a bridge. The result will clearly be planar and trivalent. It will be simple because the existence of an edge with the same endpoints would imply that some foot edge of the generalized ladder graph had endpoints in the same ladder. The existence of a pair of edges with the same endpoints would imply that either some ladder wasn't maximal, or again some foot connected vertices of the same ladder. Finally, the existence of a bridge edge would imply that there was a bridge ladder in the generalized ladder graph, but this cannot be the case, by Lemma 2.3.1, since our generalized ladder graph is 3-vertex-connected.  $\square$

An example of this correspondence between a generalized ladder graph and a simple planar trivalent graph is shown in Figure 21.

Recall that the set of crusstaceans is exactly the set of 3-vertex-connected simple planar trivalent graphs. The preceding proposition then serves as a way to characterize the set of crusstaceans that allow balanced spanning forests (with all trees with more than one edge) that give the same gluing pattern as a perfect matching, with a few minor exceptions. These exceptions are  $K_4$ , as described in Proposition 2.2.2, and the case where our graph has a single ladder. The single ladder case is addressed in the next section.

Finally, we want to emphasize that this application of perfect matchings on

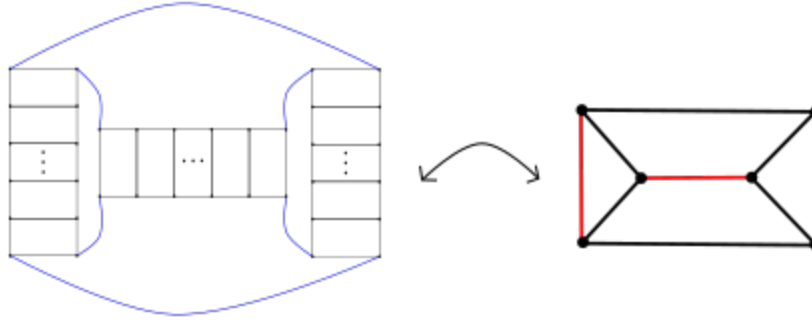


Figure 21: The correspondence between a generalized ladder graph and a simple planar trivalent graph with a perfect matching (in red).

simple planar trivalent graphs is distinct from how we have used them before. This application describes a method to characterize generalized ladder graphs, while the former application describes the balanced spanning forest associated with an FAL.

### 3 Prism Graphs and Pretzel Links

This section focuses on applications to a family of FALs called fully augmented pretzel links. Subsection 3.1 describes a family of nested links with complements homeomorphic to the fully augmented pretzel links. The size of this family is shown to grow exponentially with the number of link components. In Subsection 3.2, we show that the fully augmented pretzel links are determined by their complements, within the class of fully augmented links.

#### 3.1 Nested Links with the Complement of $S^3 \setminus \mathcal{P}_n$

In this section, we'll look at the prism graphs,  $P_n$  with  $2n$  vertices. These are of interest because they are the only 3-vertex-connected generalized ladder graphs with one ladder. The fully augmented link associated with  $P_n$  and the canonical perfect matching is what is sometimes referred to as the fully augmented pretzel link with  $n$  crossing circles, which we'll denote  $\mathcal{P}_n$ . Some properties of the fully augmented pretzel links are explored by Meyer, Millichap and Trapp in [8]. The prism graph  $P_n$  and the fully augmented pretzel link  $\mathcal{P}_n$  are shown in Figure 22.

We would like to consider nested links with the same complement as  $\mathcal{P}_n$ . We will need to be able to determine when two balanced spanning forests on  $P_n$  that give the same gluing pattern as the canonical perfect matching are associated with two different links. We'll introduce some tools that will help us do this.

If  $c_1$  and  $c_2$  denote two components in a given link, let  $lk(c_1, c_2)$  denote the

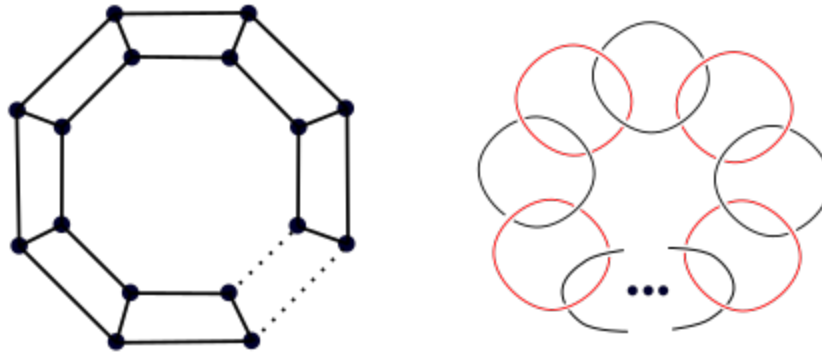


Figure 22: Left: The prism graph  $P_n$ . Right: The fully augmented pretzel link  $\mathcal{P}_n$ .

linking number of  $c_1$  and  $c_2$ , where linking number is defined in the usual way, as in [12], where it is shown to be an isotopy invariant for corresponding components. For our purposes, it suffices to know that  $lk(c_1, c_2) \neq 0$  if and only if  $c_1$  and  $c_2$  are nontrivially linked with one another. Then, given a link, we can associate a graph called the *linking graph*. In this graph, each vertex  $v_i$  corresponds to a link component  $c_i$ , and there is an edge connecting vertices  $v_i$  and  $v_j$  if and only if  $lk(c_i, c_j) \neq 0$ . Note that isotopic links must have isomorphic linking graphs.

We also define the *component linking number* of a link component to be the number of other components with which it is nontrivially linked. We denote the component linking number of a component  $c_i$  as  $cln(c_i)$ . We note that in our context  $cln(c_i)$  is equal to the degree of the corresponding vertex in the linking graph.

We would like to consider balanced trees with three edges on  $P_n$  that give the same gluing pattern as the canonical perfect matching. We assign one direction to traverse the paths of rails as “clockwise.” We’ll then use binary digits to distinguish between the two types of trees with three edges: we associate a 0 with such a tree where the edge of symmetry is on the counter-clockwise side of the rail edges in the tree, and a 1 with such a tree where the edge of symmetry is on the clockwise side of the rail edges in the tree. An example of coloring  $P_6$  in this way is given in Figure 23.

We’ll use the term *primary crossing circle* to refer to the crossing circles associated with the edge of symmetry in the tree on the crustacean. When each tree has three edges, these will be the only crossing circles whose associated crossing disks are punctured by another crossing disk. We’ll also use the term *primary knot circle* to refer to knot circles that link two different primary crossing circles. Equivalently, the primary knot circles are the components associated with the feet that connect distinct sub-ladders in  $P_n$ .

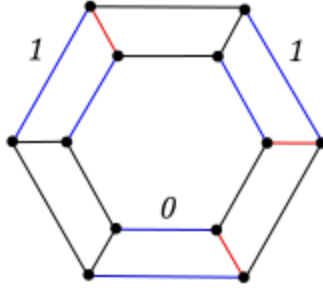


Figure 23: Example  $P_6$  Coloring

**Lemma 3.1.1.** *Consider the link formed from a balanced spanning forest on  $P_n$  that gives the canonical gluing pattern. Suppose that on some connected sub-ladder two consecutive trees in the forest are composed of three edges. Then, the primary crossing circles associated with these trees each have a component linking number of three. Further, if in clockwise order we have*

- i. a 0 tree followed by a 0 tree or a 1 tree followed by a 1 tree, then the associated primary knot circle has component linking number 3.*
- ii. a 0 tree followed by a 1 tree, then the associated primary knot circle has component linking number 4.*
- iii. a 1 tree followed by a 0 tree, then the associated primary knot circle has component linking number 2.*

*Finally, any other components associated with this subgraph have a component linking number of 2.*

*Proof.* We'll use Figure 24 to address all cases.

The images in Figure 24 depict the four options for two consecutive trees, each with three edges along with the tangles associated with each option. In the diagrams, the primary crossing circles are in red and the primary knot circles are in green. In each of these cases, since each tree corresponds to two pairs of vertices being glued, we know that each primary crossing disk is punctured by one knot circle and one crossing disk. Thus, each primary crossing circle links with the primary knot circle in addition to each of the knot circles that puncture the nested crossing circle. Thus, indeed, each primary crossing circle has component linking number 3.

We can also see that the non-primary knot circles each link with two crossing circles and the non-primary crossing circles link with two knot circles.

Finally, we consider the primary knot circles. The diagrams clearly show that the component linking numbers for each of these components is as expected.  $\square$

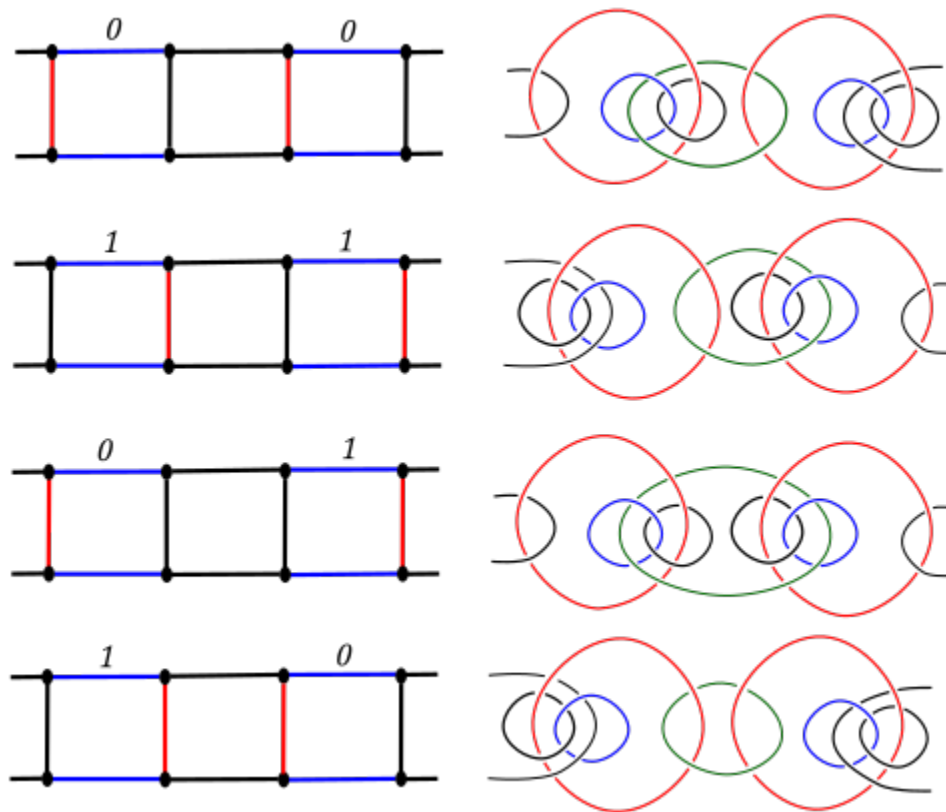


Figure 24: The four options for two consecutive trees with three edges.

**Theorem 3.1.2.** *For even  $n$ , there are at least  $2^{n/2}/n$  distinct nested links whose complement is homeomorphic to that of  $\mathcal{P}_n$ .*

*Proof.* Let  $P_n$  have a balanced spanning forest such that each tree has three edges and the gluing pattern is the same as that given by the canonical perfect matching in  $P_n$ . Then, it follows from Theorem 2.2.3 that the complement of the nested link associated with  $P_n$  has the same complement as  $\mathcal{P}_n$ .

By Lemma 3.1.1, the primary crossing circles must have a component linking number of 3 and link with exactly two primary knot circles. Further, if any other components have a component linking number of 3, each must be a primary knot circle. Note that primary knot circles link with exactly two distinct primary crossing circles and that the sublink composed of primary crossing circles and primary knot circles forms a chain. Since component linking number is equal to the degree of the associated vertex in the linking graph, we have shown that there is a unique cycle in the linking graph where (at least) every other vertex has degree 3, given by vertices associated with primary crossing circles and primary knot circles, alternating. We'll look at the degree sequence along this cycle, which has length  $n$ .

If every vertex along this cycle has degree 3, then the crustacean must be covered by all 0 trees or all 1 trees. Now, assume that not every vertex in this cycle has degree 3. Then, the vertices associated with primary crossing circles can be determined, since these all have degree 3 and alternate with the primary knot circles. Let's consider the subsequence given by the degrees of the primary knot circles. This subsequence will have length  $n/2$ , since every other vertex along the originally identified cycle is associated to a primary knot circle. We can traverse this subsequence in two directions. In each direction, we can associate an  $n/2$  length cycle of binary digits, since the degree sequence of these vertices tells us when we change between 0 trees and 1 trees. Further, every binary cycle has an associated degree sequence of this form. There are  $2^{n/2}$  binary strings of length  $n/2$  and at most  $n/2$  can correspond to the same cycle, so there are at least  $2^{n/2}/(n/2)$  distinct binary cycles. In general, traversing the degree sequence in different directions will yield distinct binary cycles, so since there were two ways to traverse our degree sequence, we can say that there are at least  $2^{n/2}/n$  binary cycles associated with distinct degree sequences.  $\square$

Note that this lower bound is not sharp. This argument can easily be extended by considering forests containing trees of depth other than two. Arguments can be made related to integer partitions of  $n$ . In this way, we can also consider odd  $n$ . The above argument is made to show that this value is at least exponential in  $n/2$ .

Theorem 2.2.3 tells us that all of these nested links are related by some sequence of Dehn twists. By the work of Whitehead, we know that, in general, we can use Dehn twists to generate infinitely many distinct links with homeomorphic complements [14]. Note, however, that we cannot continue to perform Dehn twists indefinitely and still be left with a nested link; this follows from the fact that there

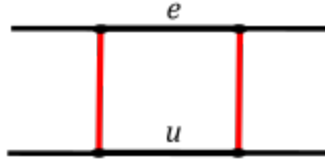


Figure 25: Two edges corresponding to one knot circle.

are only finitely many nested links with the same number of components.

### 3.2 Fully Augmented Pretzel Links

We end this section by taking a closer look at the fully augmented pretzel links.

**Lemma 3.2.1.** *The fully augmented pretzel links  $\mathcal{P}_n$  ( $n \geq 3$ ) are the only flat hyperbolic FALs with the same number of crossing circles and knot circles.*

*Proof.* First, note that there are no hyperbolic FALs with only one crossing disk. Now, consider a hyperbolic FAL with two crossing disks. The crusstacean for this link must have four vertices and must thus be  $K_4$ . Up to a rotation or reflection, there is only one perfect matching on  $K_4$ . This painting gives the Borromean rings which only has one knot circle. Thus, there are no flat hyperbolic FALs with one or two crossing circles and the same number of knot circles.

Now, suppose we have a flat hyperbolic FAL with  $n$  crossing circles and  $n$  knot circles, for  $n \geq 3$ . The crusstacean of such an FAL must have  $2n$  vertices, since there are  $n$  edges in the perfect matching. Then, the degree sum formula tells us that we must have  $3n$  edges. Of those edges,  $n$  lie in the perfect matching, and thus there must be exactly  $2n$  uncolored edges. Recall that these uncolored edges will correspond to the knot circles.

Note that our crusstaceans are all simple graphs, so there are no double edges. Therefore, a single edge in the crusstacean of an FAL cannot correspond to a single knot circle. We can then see that for each knot circle, there must be exactly two corresponding edges in the crusstacean. In the crusstacean of a flat FAL, a pair of uncolored edges  $e, u$  can correspond to a single knot circle only if each of the endpoints of  $e$  is glued to one of the endpoints of  $u$ . This only occurs if  $e$  and  $u$  connect opposite ends of a pair of edges in a perfect matching, as in Figure 25. Every uncolored edge has a partner uncolored edge that satisfies the same property as just described. The structure of our graph then continues in this manner and forms  $P_n$  with the canonical perfect matching, which is the painted crusstacean for  $\mathcal{P}_n$ .  $\square$



Note that this proof also tells us that  $P_n$  with the canonical perfect matching is the unique crusstacean for  $\mathcal{P}_n$ .

Before proceeding to the statement and proof of the next theorem, we want to recall that Mostow's rigidity theorem tells us that geometric properties of finite-volume hyperbolic 3-manifolds are in fact topological invariants. In particular, the number of cusps and the volume of a hyperbolic link complement are topological invariants.

**Theorem 3.2.2.** *Within the class of hyperbolic flat FALs, the fully augmented pretzel links  $\mathcal{P}_n$  are uniquely determined by their complements.*

*Proof.* First, note that for each component in a hyperbolic link, there is an associated cusp in the complement. The number of cusps of a hyperbolic 3-manifold is a topological invariant, so if two hyperbolic links have homeomorphic complements, they must have the same number of components.

Suppose we have a hyperbolic flat FAL  $F$  whose complement is homeomorphic to that of  $\mathcal{P}_n$ . Note that  $\mathcal{P}_n$  has  $2n$  components, so we have shown  $F$  must have  $2n$  components. We know that the number of crossing circles for any fully augmented link must be greater than or equal to the number of knot circles, so if  $F$  is distinct from  $\mathcal{P}_n$ , then  $F$  must have at least  $n + 1$  crossing circles, by Lemma 3.2.1. Our goal is to show that this cannot be the case, given that  $S^3 \setminus F$  is homeomorphic to  $S^3 \setminus \mathcal{P}_n$ .

In [10], Purcell states that if  $F$  has  $c$  crossing circles, then the hyperbolic volume of  $F$  is at least  $2v_8(c - 1)$  where  $v_8 = 3.66386\dots$  is the volume of a regular ideal tetrahedron. We note that this lower bound is increasing with the number of crossing circles, so the lower bound for more than  $n + 1$  crossing circles is greater than the lower bound for  $n + 1$  crossing circles. We can then say that a fully augmented link with at least  $n + 1$  crossing circles has volume at least  $2n \cdot v_8$ . We'll denote this lower bound  $lb(n + 1) = 2n \cdot v_8$ .

Now, we want to consider the volume of  $S^3 \setminus \mathcal{P}_n$ . Let  $\mathcal{L}(\theta) = -\int_0^\theta \ln|2\sin(x)|dx$ . Then, Thurston proves in [13] that  $vol(S^3 \setminus \mathcal{P}_n) = 8n(\mathcal{L}(\frac{\pi}{4} + \frac{\pi}{2n}) + \mathcal{L}(\frac{\pi}{4} - \frac{\pi}{2n}))$ . In [8], Meyer, Millichap and Trapp use this formula to prove that  $\frac{vol(S^3 \setminus \mathcal{P}_n)}{2n}$  is strictly increasing and  $\lim_{n \rightarrow \infty} \frac{vol(S^3 \setminus \mathcal{P}_n)}{2n} = v_8$ . Clearly,  $\frac{lb(n+1)}{2n} = \frac{2n \cdot v_8}{2n} = v_8$  for all  $n$ . This shows that for all  $n$ ,  $vol(S^3 \setminus \mathcal{P}_n) < lb(n + 1)$ . Thus, if  $L$  has  $n + 1$  or more crossing circles, then its complement cannot be homeomorphic to that of  $\mathcal{P}_n$ .  $\square$

## 4 Directions for Further Work

The crusstacean is a graph that contains a lot of information about the complements of nested links. A more thorough description of the correspondence between nested links and their crusstaceans is desirable. One could also examine how certain paths in the crusstacean correspond to components in the corresponding link.

An earlier version of this paper utilized a “fact” that if two balanced spanning forests on a cruschacean gave the same gluing pattern, then the nested links associated with these balanced spanning forests must have homeomorphic complements. The reasoning follows from the correspondence between glued vertices and glued faces in the cell decomposition. Theorem 2.2.3 proves this for some cases, but a rigorous proof of the more general statement should be given elsewhere.

Finally, it has been conjectured that all FALs are uniquely determined by their complements within the class of fully augmented links. Theorem 3.2.2 proves this for the subclass of fully augmented pretzel links, but it does not seem likely that this particular method will generalize.

## Acknowledgements

I’d like to thank Dr. Fred Cohen for advising this project as a senior thesis. I’d also like to thank Dr. Rollie Trapp for initially advising this work as an REU. Finally, I would like to thank California State University, San Bernardino and NSF grant DMS-1758020 for partially funding this work.

## References

- [1] Eric Chesebro, Jason DeBlois, and Henry Wilton. “Some virtually special hyperbolic 3-manifold groups”. In: *Comment. Math. Helv.* 87.3 (2012), pp. 727–787. ISSN: 0010-2571. DOI: 10.4171/CMH/267.
- [2] Maria Chudnovsky and Paul Seymour. “Perfect matchings in planar cubic graphs”. In: *Combinatorica* 32.4 (2012), pp. 403–424. ISSN: 0209-9683. DOI: 10.1007/s00493-012-2660-9.
- [3] Tomotaka Fukuda, Seiya Negami, and Thomas W. Tucker. “3-connected planar graphs are 2-distinguishable with few exceptions”. In: *Yokohama Math. J.* 54.2 (2008), pp. 143–153. ISSN: 0044-0523.
- [4] C. McA. Gordon and J. Luecke. “Knots are determined by their complements”. In: *J. Amer. Math. Soc.* 2.2 (1989), pp. 371–415. ISSN: 0894-0347. DOI: 10.2307/1990979.
- [5] John Harnois, Hayley Olson, and Rolland Trapp. “Hyperbolic tangle surgeries and nested links”. In: *Algebr. Geom. Topol.* 18.3 (2018), pp. 1573–1602. ISSN: 1472-2747. DOI: 10.2140/agt.2018.18.1573.
- [6] Marc Lackenby. “The volume of hyperbolic alternating link complements”. In: *Proc. London Math. Soc. (3)* 88.1 (2004). With an appendix by Ian Agol and Dylan Thurston, pp. 204–224. ISSN: 0024-6115. DOI: 10.1112/S0024611503014291. URL: <https://doi.org/10.1112/S0024611503014291>.

- [7] Brian Mangum and Theodore Stanford. “Brunnian links are determined by their complements”. In: *Algebr. Geom. Topol.* 1 (2001), pp. 143–152. ISSN: 1472-2747. DOI: 10.2140/agt.2001.1.143.
- [8] Jeffrey Meyer, Christian Millichap, and Rolland Trapp. “Arithmeticity and Hidden Symmetries of Fully Augmented Pretzel Link Complements”. In: *arXiv: Geometric Topology* (Nov. 2018).
- [9] Hayley Olsen. *Nested and Fully Augmented Links*. CSUSB Mathematics REU, 2016.
- [10] Jessica S. Purcell. “An introduction to fully augmented links”. In: *Interactions between hyperbolic geometry, quantum topology and number theory*. Vol. 541. Contemp. Math. Amer. Math. Soc., Providence, RI, 2011, pp. 205–220. DOI: 10.1090/conm/541/10685.
- [11] Jessica S. Purcell. *Hyperbolic Knot Theory*. 2020. arXiv: 2002.12652 [math.GT].
- [12] Saul Stahl and Catherine Stenson. *Introduction to topology and geometry*. Second. Pure and Applied Mathematics (Hoboken). John Wiley & Sons, Inc., Hoboken, NJ, 2013, pp. xvi+512.
- [13] William Thurston. *The Geometry and Topology of 3-Manifolds*. Lecture Notes. 1978.
- [14] J. H. C. Whitehead. “On Doubled Knots”. In: *Journal of the London Mathematical Society* s1-12.1 (1937), pp. 63–71. DOI: 10.1112/jlms/s1-12.45.63.
- [15] Hassler Whitney. “Congruent Graphs and the Connectivity of Graphs”. In: *Amer. J. Math.* 54.1 (1932), pp. 150–168. ISSN: 0002-9327. DOI: 10.2307/2371086.